2015 European Control Conference (ECC)
July 15-17, 2015. Linz, Austria

A Globally Exponentially Stable filter for Bearing-Only Simultaneous Localization and Mapping in 3-D

Pedro Lourenço, Pedro Batista, Paulo Oliveira, and Carlos Silvestre

Abstract— **This paper proposes a novel filter for sensor-based bearing-only simultaneous localization and mapping in three dimensions with globally exponentially stable (GES) error dynamics. A nonlinear system is designed, its output transformed, and its dynamics augmented so that the proposed formulation can be considered as linear time-varying for the purpose of observability analysis. This allows the establishment of observability results related to the original nonlinear system that naturally lead to the design of a Kalman filter with GES error dynamics. The performance of the proposed algorithm is assessed resorting to a set of realistic simulations.**

I. Introduction

Navigation using directions to known sources has been in use for centuries. Initially, in marine applications, several tools to measure the elevation of stars such as sextants and mariner's astrolabes were employed to derive the position of ships, and lighthouses were used in triangulation techniques. In the last century, aviation brought into use more advanced technologies supported on bearings (azimuth and/or elevation) readings: the automatic direction finder (ADF), the VHF omnidirectional range (VOR), and the instrument landing system (ILS) are the most common still in use today. The advent of global positioning systems has gradually replaced the use of these techniques, but in GPS-denied environments, aided relative algorithms are still called for to navigate unmanned vehicles. A family of algorithms that addresses this issue is simultaneous localization and mapping (SLAM), a concept introduced in the scientific community in the 1980's [1] and first coined in [2].

The most studied version of the SLAM problem is what is called range-bearing SLAM, where the coordinates of measured landmarks are readily available (see [3] and [4] for a survey on this subject). This is known in the scientific community as fully observable SLAM, as a single measurement is sufficient to estimate landmark positions. However, there are versions of the problem that omit one of the two informations available, either range-only SLAM (RO-SLAM) or bearing-only SLAM (BO-SLAM). These approaches are named partially-observable, as a single noise-free observation provides only a line or surface as an estimate for the position of a landmark. The bearing-only case is even more difficult to treat than the range-only one, because an observation corresponds to an unbounded region. This raises serious issues on the initialization of a landmark, which has been the main topic of research in partially-observable SLAM, yielding mostly delayed solutions, i.e., algorithms that try to obtain a preliminary landmark estimate from readings at different viewpoints before introducing the initial estimate in the filter. This can be done through triangulation or more advanced probabilistic approaches, using, for example, a sum of Gaussians [5] or deterring the initialization until an approximately Gaussian estimate is achieved [6]. There are some notable exceptions in [7] and [8] that recur to multiple hypothesis directly in the filter. Other common trait in this field is the scarcity of tridimensional algorithms.

Although research in BO-SLAM is not as prolific as it is in range-bearing SLAM, the community has provided several approaches depending on the underlying filtering technique and the sensors used. Most algorithms are based on extended kalman filters (EKF). However, some methods are inspired on expectation-maximization or particle filters (see [9] for a comparison of these approaches). Another source of diversity in BO-SLAM algorithms is the type of sensor used. Even though bearing-only localization is historically related to the computation of the angle-of-arrival of signals from beacons through the time difference of arrival at different elements of a receiving array, BO-SLAM is mostly associated with monocular vision [10] or even catadioptric omnidirectional systems [11].

One of the greatest problems in any SLAM framework is data association. In range-bearing SLAM this issue is mostly solved and there are several different algorithms that tackle it. In BO-SLAM, however, there are extra difficulties in the initialization process. Some approaches try to deal with all hypothesis when initializing [12], but vision-based algorithms may use image information if the frame-rate is high enough to disambiguate measurements. Data association is not within the scope of this paper, and therefore the measurements are assumed to be perfectly associated with the corresponding state. This is not a troublesome assumption as the bearings may be obtained from tagged signals coming from beacons, for instance.

This work was supported by the Fundação para a Ciência e a Tecnologia (FCT) through ISR under LARSyS UID/EEA/50009/2013, and through IDMEC, under LAETA UID/EMS/50022/2013 projects, and by the University of Macau MYRG117(Y1-L3)-FST12-MKM project. The work of P. Lourenço was supported by the PhD Student Grant SFRH/BD/89337/2012 from FCT.

The authors are with the Institute for Systems and Robotics, Laboratory of Robotics and Systems in Engineering and Practice, Portugal. P. Batista is also with Instituto Superior Técnico, Universidade de Lisboa, Portugal. P. Oliveira is also with the Department of Mechanical Engineering, Instituto Superior Técnico, Universidade de Lisboa, Portugal. C. Silvestre is with the Department of Electrical and Computer Engineering of the Faculty of Science and Technology of the University of Macau, Macao, China, on leave from Instituto Superior Técnico, Universidade de Lisboa, Lisbon, Portugal.
{plourenco,pbatista,pjcro,cjs}@isr.ist.utl.pt

This work solves the initialization problem by introducing a BO-SLAM algorithm with exponentially fast global convergence, which allows for undelayed initialization at any depth. With its tridimensional (3-D) sensor-based approach, the pose of the vehicle is eliminated from the filter state and the inclusion of odometry-like measurements and relative bearings is straightforward. This aspect, coupled with a state augmentation and output transformation, leads to the design of an LTV system whose observability is analysed in this paper, resulting in constructive conditions with clear physical insight that are important for motion planning. The theoretical results are complemented by meaningful and realistic simulations. The underlying idea of this paper is influenced by the source-localization algorithm presented in [13], as the proposed filter results from similar state and output transformations.

II. The bearing-only SLAM problem

Consider a vehicle operating in a static environment, capable of measuring the relative azimuth and elevation of landmarks installed in unknown locations, as well as its linear and angular velocities in its own reference frame. The landmarks can be artificial or natural, i.e., previously installed or extracted from the scenery. This situation falls under the scope of BO-SLAM, which is the problem of navigating a vehicle in an unknown environment, building a map of metric landmarks by measuring bearings and using this map to deduce its location, without the need for *a priori* information about landmark inertial location.

A. The sensor-based approach

The sensor-based approach, or, as it is commonly known in the SLAM community, the robocentric approach to SLAM has been proven more consistent than its inertial, world-centric, counterpart [14]. Furthermore, previous observability studies using piece-wise linearizations showed that this approach becomes fully observable in two time steps, in opposition to what happens in the world-centric case [15]. In addition, in this family of problems where the measurements are all expressed in local coordinates it makes sense to operate in a sensor-based framework, as it is a way of avoiding the inclusion of the pose of the vehicle in the filter state, one of the main sources of nonlinearity. That is the idea behind the nonlinear system that underlies the filter to be detailed. However, inertial estimates can still be obtained using an algorithm such as the one proposed in [16] or, using at least two landmarks as anchors with known coordinates.

Recall the situation described above, and consider two different reference frames. One fixed to the vehicle, denoted as body-fixed frame $\{B\}$, and the other fixed in the environment, denoted as the inertial frame $\{I\}$. The two frames are related through the rotation matrix $\mathbf{R}(t) \in \mathrm{SO}(3)$ and the translation ${}^I\mathbf{p}(t) \in \mathbb{R}^3$. The former represents the attitude of the vehicle and satisfies $\dot{\mathbf{R}}(t) = \mathbf{R}(t)\mathbf{S}\left[\boldsymbol{\omega}(t)\right]$, where $\mathbf{S}\left[\boldsymbol{\omega}(t)\right]$ is a skew-symmetric matrix that encodes the cross-product and $\boldsymbol{\omega}(t) \in \mathbb{R}^3$ is the angular velocity of the vehicle expressed in $\{B\}$. Similarly, the translation represents the position of the vehicle in the inertial frame, coincident with the origin of the body-fixed frame expressed in $\{I\}$.

The environment, i.e., the map, consists of N static landmarks ${}^I\mathbf{p}_i(t) \in \mathbb{R}^3$ that compose the landmark set $\mathcal{L} = \{1, \ldots, N\}$. Depending on the pose of the vehicle, some of these landmarks may be visible or not, which motivates the definition of two subsets of landmarks, $\mathcal{L}_o = \{1, \ldots, N_O\}$ and $\mathcal{L}_u = \{N_O + 1, \ldots, N\}$. The first contains the N_O observed or visible landmarks while the latter contains the unobserved, or non-visible, ones. Note that, without loss of generality, the landmarks are ordered for simplicity of analysis. In the body-fixed frame, the i-th landmark is denoted by $\mathbf{p}_i(t) = \mathbf{R}^T(t)\left({}^I\mathbf{p}_i(t) - {}^I\mathbf{p}(t)\right)$ and its derivative satisfies $\dot{\mathbf{p}}_i(t) = -\mathbf{S}\left[\boldsymbol{\omega}(t)\right]\mathbf{p}_i(t) - \mathbf{v}(t)$, where $\mathbf{v}(t) \in \mathbb{R}^3$ is the linear velocity of the vehicle expressed in its own frame.

From the problem definition, it is known that both the linear and the angular velocities are measured, as well as relative bearings to the landmarks. This last quantity is described by the unit vector $\mathbf{b}_i(t)$ that defines the line between the position of the vehicle and landmark i, and is given by $\mathbf{b}_i(t) = \mathbf{p}_j(t)\|\mathbf{p}_i(t)\|^{-1}$ with $i \in \mathcal{L}_o$. As the information this measurement carries is limited, not only several measurements from the same landmark are needed to unambiguously determine its position but also some measure of scale is required. This is provided by the linear velocity measurements and it is the reason why they must be available.

This section culminates naturally with the nonlinear system that puts all this information together. The position of the landmarks in the body-fixed frame and the linear velocity are its states and the measured quantities are its outputs ($\mathbf{v}(t)$ and $\mathbf{b}_i(t)$). The linear velocity is included as a state with zero derivative for filtering purposes, even though it is measured directly. The resulting system dynamics is

$$\begin{cases} \dot{\mathbf{p}}_i(t) = -\mathbf{S}\left[\boldsymbol{\omega}(t)\right]\mathbf{p}_i(t) - \mathbf{v}(t) \\ \dot{\mathbf{v}}(t) = \mathbf{0} \\ \mathbf{b}_j(t) = \mathbf{p}_j(t)\|\mathbf{p}_j(t)\|^{-1} \\ \mathbf{y}_v(t) = \mathbf{v}(t) \end{cases} \tag{1}$$

where $i \in \mathcal{L}$ and $j \in \mathcal{L}_o$.

B. Problem statement

The problem addressed in this paper is that of designing a navigation system for a vehicle operating in the environment here described, by means of a filter for the dynamics in (1), assuming noisy measurements. The algorithm consists of a BO-SLAM filter in the space of sensors, and, therefore, the pose of the vehicle is deterministic as, by construction, it simply corresponds to the position and attitude of the body-fixed frame expressed in that same frame.

III. Proposed solution: GES BO-SLAM

The system presented in the last section is still nonlinear, even though the sensor-based approach allowed to avoid including the pose of the vehicle in the dynamics. In some problems, where the nonlinearity occurs in the output equation, a state augmentation can help to remove the nonlinearity, as was done successfully in [17], where the idea was applied to RO-SLAM. In this paper, the proposed solution relies on an output transformation that leads to a state augmentation, inspired by the results presented in [13].

A. State augmentation and output transformation

The objective of this subsection is to obtain a linear-like system that mimics the dynamics of the original nonlinear system while avoiding the nonlinearity on the bearing output. Consider then the simple manipulation of the output of (1) that yields $\mathbf{p}_i(t) - \mathbf{b}_i(t)\|\mathbf{p}_i(t)\| = \mathbf{0}$, $i \in \mathcal{L}_o$. If the norm of the i-th landmark is added as a state, this expression becomes in fact linear. That is the idea behind the augmented state $\mathbf{x}_F(t) := \begin{bmatrix}\mathbf{x}_L^T(t) & \mathbf{x}_V^T(t) & \mathbf{x}_R^T(t)\end{bmatrix}^T$, where $\mathbf{x}_L(t) \in \mathbb{R}^{n_L}$ is the stacking of all landmarks, both visible and non-visible, $\mathbf{x}_V(t) \in \mathbb{R}^3$ is the linear velocity and $\mathbf{x}_R(t) \in \mathbb{R}^{n_R}$ agglomerates all the norms of the landmarks, i.e., the range from each landmark to the vehicle. These correspondences are summarized by the state constraints

$$\begin{cases} \mathbf{x}_{L_i}(t) := \mathbf{p}_i(t) \\ \mathbf{x}_V(t) := \mathbf{v}(t) \\ x_{R_i}(t) := \|\mathbf{x}_{L_i}(t)\| \end{cases}, \tag{2}$$

for all $i \in \mathcal{L}$, where $\mathbf{x}_{L_i}(t) \in \mathbb{R}^3$ and $x_{R_i}(t) \in \mathbb{R}$ are i-th components of the landmark and range state vectors, respectively. Note that both the landmark and range states are composed by visible and non-visible parts, denoted by subscripts O and U respectively.

Consider the derivative of the range state, given by

$$\dot{x}_{R_i}(t) = -\frac{\mathbf{x}_{L_i}^T(t)}{x_{R_i}(t)}\mathbf{x}_V(t)$$

which is needed to write the full state dynamics. When a landmark is observed and its bearing is available, the quotient $\frac{\mathbf{x}_{L_i}(t)}{x_{R_i}(t)}$ can be replaced by the bearing $\mathbf{b}_i(t)$ for all $i \in \mathcal{L}_o$. Knowing this, the resulting system reads

$$\begin{cases} \dot{\mathbf{x}}_F(t) = \mathbf{A}_F(t, \mathbf{x}_{L_U}(t), \mathbf{x}_{R_U}(t))\, \mathbf{x}_F(t) \\ \mathbf{y}(t) = \mathbf{C}_F(t)\, \mathbf{x}_F(t) \end{cases}, \tag{3}$$

where the dynamics matrix is

$$\mathbf{A}_F(t, \mathbf{x}_{L_U}(t), \mathbf{x}_{R_U}(t)) = \begin{bmatrix} \mathbf{A}_L(t) & \mathbf{A}_{LV} & \mathbf{0}_{n_L \times n_R} \\ \mathbf{0}_{3\times n_L} & \mathbf{0}_{3\times 3} & \mathbf{0}_{3\times n_R} \\ \mathbf{0}_{n_R\times n_L} & \mathbf{A}_{RV}(t, \mathbf{x}_{L_U}(t), \mathbf{x}_{R_U}(t)) & \mathbf{0}_{n_R\times n_R} \end{bmatrix}$$

with components $\mathbf{A}_L(t) = -\operatorname{diag}\left(\mathbf{S}\left[\boldsymbol{\omega}(t)\right], \ldots, \mathbf{S}\left[\boldsymbol{\omega}(t)\right]\right)$, $\mathbf{A}_{LV} = -\begin{bmatrix}\mathbf{I}_3 & \cdots & \mathbf{I}_3\end{bmatrix}^T$, and

$$\mathbf{A}_{RV}(t, \mathbf{x}_{L_U}(t), \mathbf{x}_{R_U}(t)) = -\operatorname{diag}\left(\mathbf{b}_1^T(t), \ldots, \mathbf{b}_{N_O}^T(t), \frac{\mathbf{x}_{L_i}^T(t)}{x_{R_i}(t)}, \ldots, \frac{\mathbf{x}_{L_{N_O+1}}^T(t)}{x_{R_N}(t)}\right).$$

The output matrix is

$$\mathbf{C}_F(t) = \begin{bmatrix} \mathbf{0}_{3\times n_O} & \mathbf{0}_{3\times n_U} & \mathbf{I}_3 & \mathbf{0}_{3\times n_{R_O}} & \mathbf{0}_{3\times n_{R_U}} \\ \mathbf{I}_{n_O} & \mathbf{0}_{n_O\times n_U} & \mathbf{0}_{n_O\times 3} & \mathbf{C}_b(t) & \mathbf{0}_{n_O\times n_U} \end{bmatrix},$$

with $\mathbf{C}_b(t) = -\operatorname{diag}\left(\mathbf{b}_1(t), \ldots, \mathbf{b}_{N_O}(t)\right)$. Finally, the output is $\mathbf{y}(t) = \begin{bmatrix}\mathbf{v}^T(t) & \mathbf{0}_{1\times n_O}\end{bmatrix}^T$.

Even though the output nonlinearity as first brought up disappeared with the state augmentation and output transformation proposed in this section, the process introduced two new non-linearities. The first is on the dynamics matrix, as it depends both on a measured quantity, the bearing, and on the state, when the measurement is not available. The second is on the output matrix that also depends on a measured quantity. However. the presence of the measurement in the dynamics and output matrices is not really a problem, as, for observability purposes, a system whose dynamics matrix depends on the output can be seen as a linear time-varying (LTV) system. The presence of the state in the dynamics matrix only affects the non-visible landmarks ($\mathbf{x}_{L_U}(t)$ and $\mathbf{x}_{R_U}(t)$). These are not observable, and therefore will be propagated in open loop.

Another important aspect that must be stressed is the fact that the there is nothing in the augmented system (3) that imposes the constraints (2), particularly the nonlinear relation $x_{R_i}(t) = \|\mathbf{x}_{L_i}(t)\|$, and as such the relation between the nonlinear and the augmented systems must be carefully analysed.

B. Observability analysis

The subject of this subsection is the observability analysis of the nonlinear and augmented systems presented previously. The augmented system (3) contains non-visible landmarks and associated ranges that are clearly not observable as the corresponding bearing is not available. Hence, in the observability analysis, the non-visible landmarks and the associated ranges are discarded, following the successful approach first used by the authors in [18] and [19]. Furthermore, the fact that each landmark-range-bearing group is independent of the others allows to consider that only one landmark is visible, i.e., $\mathcal{L}_o := \{1\}$, which simplifies the analysis greatly.

The new reduced system is given by

$$\begin{cases} \dot{\mathbf{x}}(t) = \mathbf{A}(t)\mathbf{x}(t) \\ \mathbf{y}(t) = \mathbf{C}(t)\mathbf{x}(t) \end{cases} \tag{4}$$

where the dynamics matrix is

$$\mathbf{A}(t) = \begin{bmatrix} -\mathbf{S}\left[\boldsymbol{\omega}(t)\right] & -\mathbf{I}_3 & \mathbf{0}_{3\times 1} \\ \mathbf{0}_3 & \mathbf{0}_3 & \mathbf{0}_{3\times 1} \\ \mathbf{0}_{1\times 3} & -\mathbf{b}_1^T(t) & 0 \end{bmatrix},$$

the output matrix is

$$\mathbf{C}(t) = \begin{bmatrix} \mathbf{0}_{3\times 3} & \mathbf{I}_3 & \mathbf{0}_{3\times 1} \\ \mathbf{I}_3 & \mathbf{0}_3 & \mathbf{b}_1(t) \end{bmatrix}.$$

The dependence of the dynamics matrix on the non-visible landmarks and ranges has disappeared with the reduction of the state of this system. However, both the dynamics and the output matrices still depend on the visible bearing. Given that this quantity is a known function of time, the reduced system can be considered as linear time-varying for observability analysis and observer design. In fact, as shown in [20, Lemma 1], if the observability Gramian associated with a system whose dynamics matrix depends on the system input and output is invertible, then the system is observable. This result will be exploited throughout this subsection.

The forthcoming analysis requires the definition of ${}^I\mathbf{b}_1(t) = \mathbf{R}(t)\mathbf{b}_1(t)$ as the inertial or absolute bearing, as well as the following physically sensible assumption.

Assumption 1: The position of the vehicle cannot coincide with a landmark, i.e., a visible bearing vector is always defined.

This theorem addresses the observability analysis of system (4) regarded as LTV.

Theorem 1: Take system (4), regarded as LTV, and let $\mathcal{T} := [t_0, t_f]$. The system is observable in $\mathcal{T}$ if the absolute bearing associated with the visible landmark is not constant in $\mathcal{T}$, i.e., there exists a $t_1 \in \mathcal{T}$ such that ${}^I\dot{\mathbf{b}}_1(t_1) \neq 0$.

Proof: Consider the Lyapunov transformation (see [21] for details) $\mathbf{z}(t) = \mathbf{T}(t)\mathbf{x}(t)$, where $\mathbf{T}(t) = \operatorname{diag}(\mathbf{R}(t), \mathbf{I}_3, 1)$, which preserves the observability properties of the original system. It is a simple matter of computation to obtain the transformed system, given by

$$\begin{cases} \dot{\mathbf{z}}(t) = \boldsymbol{\mathcal{A}}(t)\mathbf{z}(t) \\ \mathbf{y}(t) = \boldsymbol{\mathcal{C}}(t)\mathbf{z}(t) \end{cases}$$

where the dynamics matrix is

$$\boldsymbol{\mathcal{A}}(t) = \begin{bmatrix} \mathbf{0}_{3\times3} & -\mathbf{R}(t) & \mathbf{0}_{3\times1} \\ \mathbf{0}_{3\times3} & \mathbf{0}_{3\times3} & \mathbf{0}_{3\times1} \\ \mathbf{0}_{1\times3} & -\mathbf{b}_1^T(t) & 0 \end{bmatrix}$$

and the output matrix is

$$\boldsymbol{\mathcal{C}}(t) = \begin{bmatrix} \mathbf{0}_{3\times3} & \mathbf{I}_3 & \mathbf{0}_{3\times1} \\ \mathbf{R}^T(t) & \mathbf{0}_3 & \mathbf{b}_1(t) \end{bmatrix}.$$

The proof, made by contraposition, follows with the transformed system for simplicity of analysis. This system is assumed not observable, which, using [20, Lemma 1] implies that the observability Gramian is singular. Then it is shown that the conditions of the theorem cannot hold. A similar proof can be found in [17]. ∎

Remark 1: The sufficient condition introduced by this theorem is in fact a requirement on the motion of the vehicle. For the system to be observable, i.e., in order to be possible to obtain the initial condition of a landmark, the trajectory of the vehicle must not be restricted to the line described by the absolute bearing.

This theorem established sufficient conditions for the observability of the system (4) that is a reduced version of the augmented nonlinear system (3). Given that the discarded states are not observable and do not influence the others, the two systems are equivalent in what concerns observability, when discarding the non-visible landmarks. Hence, this result also applies to the augmented system.

As to the original nonlinear system, this observability result cannot be extrapolated without special attention. Recall that although the augmented system (3) mimics the dynamics of the nonlinear one, there is nothing imposing the state relations (2). The sequel addresses this aspect, following the approach in previous works such as [13] and [17].

Theorem 2: If the conditions of Theorem 1 hold, then:

(i) the state of the original nonlinear system (3) and that of the LTV system (4) are the same and uniquely determined, and the constraints (2) are imposed by the dynamics;

(ii) an observer for the LTV system with globally exponentially stable error dynamics is also a state observer for the underlying nonlinear system with error dynamics that converge exponentially.

Proof: The proof of the first part of the theorem is made by considering the system output and its relation to the states of the two systems in analysis, leading to a series of equations which, in the conditions of the theorem, result in the correspondence between the states. A similar proof can be found in detail [17], along with a proof for the second part of the theorem. ∎

C. Filter design

The results of the previous subsection show that, in certain conditions with physical insight, the augmented system is equivalent to the nonlinear system, and that if a filter with GES error dynamics can be constructed to the LTV system, it will also be applicable to the original nonlinear system. It can be shown that the error dynamics of the linear time-varying Kalman filter are globally exponentially stable if the pair $(\mathbf{A}(t), \mathbf{C}(t))$ is uniformly completely observable, a form of observability stronger than the ones addressed previously. This result can be achieved following the steps in [22, Example 8.5] and [23]. This last theorem addresses the uniform complete observability of the LTV system.

Theorem 3: Let $\mathcal{T}_\delta := [t, t+\delta]$. The pair $(\mathbf{A}(t), \mathbf{C}(t))$ associated with the system (4), regarded as LTV, is uniformly completely observable if there exist positive constants δ and α_b such that, for all $t \geq t_0$, it is possible to find a $t_1 \in \mathcal{T}_\delta$ for which the absolute bearing to the visible landmark respects

$$\left\| \int_t^{t_1} {}^I\dot{\mathbf{b}}_1(\tau)\mathrm{d}\tau \right\| \geq \alpha_b.$$

Proof: The proof follows steps similar to those of Theorem 1 and is omitted. However, the reader is referred to [17] for a similar proof with slightly different dynamics. ∎

An LTV Kalman filter can now be implemented for the LTV system, and it is done so in its discrete version. Considering additive disturbances, the discretized system for time-steps of length T_s is given by

$$\begin{cases} \mathbf{x}_{F_{k+1}} = \mathbf{F}_{F_k}\mathbf{x}_{F_k} + \boldsymbol{\xi}_k \\ \mathbf{y}_{k+1} = \mathbf{C}_{F_{k+1}}\mathbf{x}_{F_{k+1}} + \boldsymbol{\theta}_{k+1} \end{cases},$$

where the dynamics matrix is

$$\hat{\mathbf{F}}_{F_k} = \begin{bmatrix} \mathbf{F}_{L_k} & T_s\mathbf{A}_{LV} & \mathbf{0}_{n_L\times n_R} \\ \mathbf{0}_{3\times n_L} & \mathbf{I}_3 & \mathbf{0}_{n_L\times n_R} \\ \mathbf{0}_{n_R\times n_L} & T_s\mathbf{A}_{RV_k} & \mathbf{I}_{n_R} \end{bmatrix},$$

with $\mathbf{F}_{L_k} = \text{diag}\left(\mathbf{R}_{k+1}^T\mathbf{R}_k, \ldots, \mathbf{R}_{k+1}^T\mathbf{R}_k\right)$ and $\mathbf{R}_{k+1}^T\mathbf{R}_k = \mathrm{e}^{-\mathbf{S}[\boldsymbol{\omega}_k]T_s}$. The vectors $\boldsymbol{\xi}_k$ and $\boldsymbol{\theta}_k$ represent the model disturbance and measurement noise, respectively. They are assumed to be zero-mean discrete white Gaussian noises with covariances $\boldsymbol{\Xi}_k$ and $\boldsymbol{\Theta}_k$. The prediction and update equations are the standard LTV Kalman filter equations [24], with one detail regarding the non-visible landmarks which must be propagated in open loop. The propagation of $x_{R_{ik}}$ for all $i \in \mathcal{L}_u$ was chosen to follow the gradient of

$$x_{R_{i_{k+1}}} = x_{R_{i_k}} + T_s \frac{\mathbf{x}_{L_{i_k}}^T \mathbf{v}_k}{x_{R_{i_k}}}.$$

In this implementation of the algorithm, the bearing measurements are assumed to carry some kind of tag, and therefore the association of measurements with the corresponding states is trivial. Furthermore, loop closures occur automatically without any need for a special procedure.

IV. Simulation results and discussion

This section details the realistic simulations performed to validate the algorithm proposed in this paper and assess its performance. The results of a typical run in the simulated environment are presented and discussed.

a) Setup: The chosen environment tries to emulate the fifth floor of the North Tower at IST. It consists of a 16 m by 16 m by 3 m corridor. 36 landmarks where put in notable places such as corners and doors, with random heights. The aerial vehicle starts stopped at the ground, and after taking off makes several laps around the corridor. It completes a loop of 55 m in 124 s, and the total trajectory is 5 loops at 0.440 $\mathrm{m/s}$. In order to better approximate the simulation to the reality, the field of view of the vehicle was limited to 90° horizontally and vertically with a range of up to 20 m. Furthermore, the effect of walls was taken into account. This means that the landmarks are only visible during a limited period of time in each loop. The bearing measurements are obtained by rotating the true bearing about random vectors of a random zero-mean angle with Gaussian distribution with standard deviation of 1°. The remaining measurements are corrupted with additive zero mean white noise. The standard deviation of the noise corrupting the linear velocity is 0.01 $\mathrm{m/s}$, and that of the angular velocity is 0.3°/s. All measurements are obtained at 20 Hz.

b) Typical run results: Figures 1(a) and 1(b) depict the estimated map at the end of the run. The first is the top-view of the map with the 95% uncertainty ellipses in green and blue depending whether they are observed in that instant or not, including the real trajectory of the vehicle in dashed red, and the pose of the vehicle at that moment, that is represented by the yellow quadrotor. The top right figure shows the 3-D map with the real trajectory in blue, the current pose of the vehicle depicted by the yellow quadrotor and the true landmark positions at the solid dots inside the 95% ellipsoids. Note that the ellipsoids surround the true values, as they should in a consistent filter. Finally, in Fig. 1(c) the estimation error for all the 36 landmarks is shown. It can be seen that even though the initial estimate may be far off, the error will converge until after 2 laps it is under 40 centimetres depending on how long each landmark is observed.

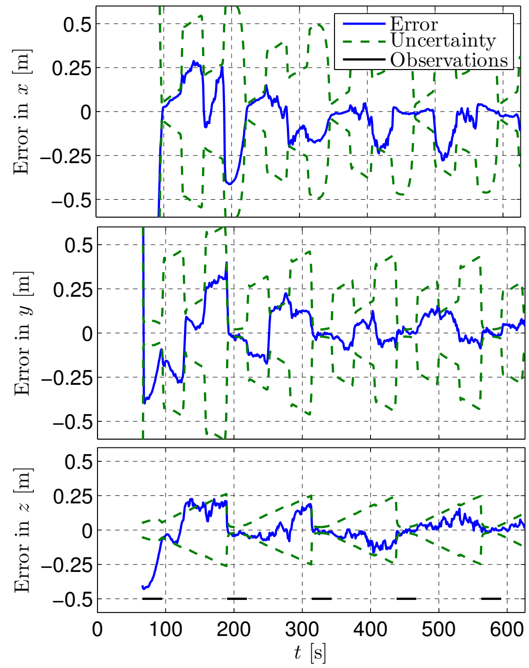

Fig. 2. The estimation error of a sensor-based landmark with 2σ uncertainty bounds and observation instants.

To provide a better understanding of the behaviour of the filter, Fig. 2 is included, where the estimation error and the 95% uncertainty bounds for all the three dimensions of one selected landmark are presented along with the moments where it was observed (black lines in the bottom graph). The convergence of the estimates is clear in this figure, as well as their consistency. Particularly, when the landmark is once more reobserved, both the error and the uncertainty decrease very fast. These results are in accordance with the theoretical guarantees presented in Section III.

V. Conclusions and future work

A novel sensor-based globally exponentially stable filter for bearing-only simultaneous localization and mapping was proposed in this paper. Making use of a state augmentation and a simple output transformation on a nonlinear system, while disposing of non-visible landmarks, paved the way for the design of a linear time-varying system that mimics the dynamics of the underlying nonlinear system. A thorough and constructive observability analysis was performed, leading to the establishment of physically-grounded sufficient conditions for observability, stability and convergence of the Kalman filter that followed. These conditions are interesting for trajectory design or motion planning. The theoretical work which is the main focus of this paper was validated through realistic simulations that demonstrated the good performance of the algorithm.

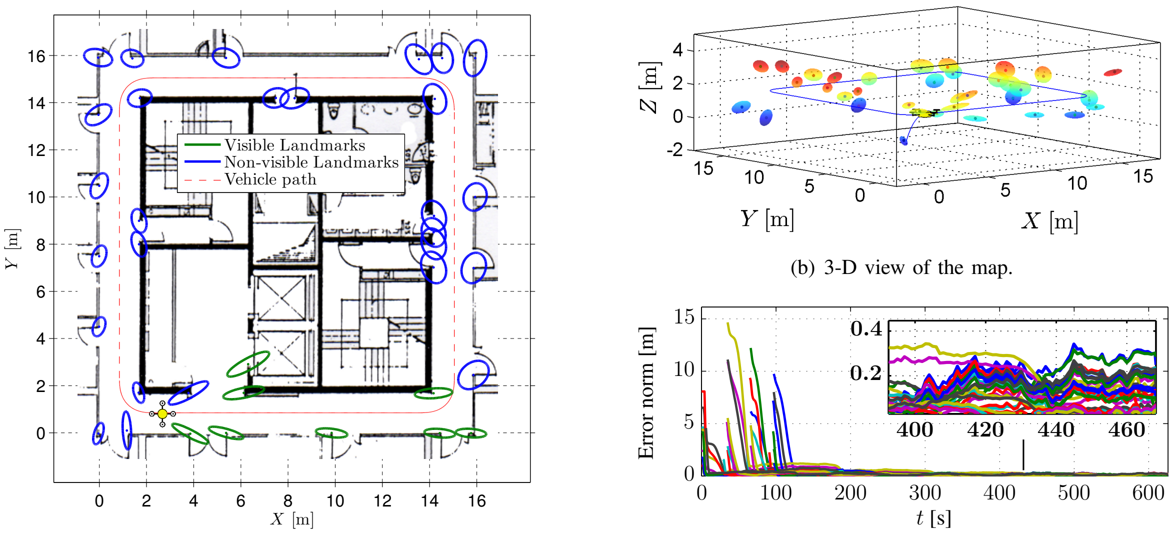

(a) Top-view of the map.

(b) 3-D view of the map.

(c) Norm of the error.

Fig. 1. The estimated landmarks. Picture of the estimated map rotated and translated using the true transformation at $t = 626$ s, with 2σ ellipsoids, on the left. Top right: 3-D map. Bottom right: the evolution of the norm of the estimation error for all the 36 landmarks.

With respect to future work, the authors identify two main courses of action. First, the extension of the observability analysis to obtain necessary conditions, and second, the experimental validation of the algorithm with an aerial vehicle equipped with an array of receivers and an environment composed of a constellation of beacons.

References

[1] R. Smith and P. Cheeseman, "On the representation and estimation of spatial uncertainty," *International Journal of Robotics Research*, vol. 5, no. 4, pp. 56–68, Dec. 1986.

[2] J. Leonard and H. Durrant-Whyte, "Simultaneous map building and localization for an autonomous mobile robot," in *Proc. of the IEEE/RSJ International Workshop on Intelligent Robots and Systems (IROS)*, vol. 3, 1991, pp. 1442–1447.

[3] H. Durrant-Whyte and T. Bailey, "Simultaneous Localisation and Mapping (SLAM): Part I The Essential Algorithms," *IEEE Robotics & Automation Magazine*, vol. 13, no. 2, pp. 99–110, 2006.

[4] T. Bailey and H. Durrant-Whyte, "Simultaneous localization and mapping (SLAM): Part II," *IEEE Robotics & Automation Magazine*, vol. 13, no. 3, pp. 108–117, 2006.

[5] T. Lemaire, S. Lacroix, and J. Solà, "A practical 3D bearing-only SLAM algorithm," in *Proceedings of the 2005 IEEE/RSJ International Conference on Intelligent Robots and Systems*, Aug 2005, pp. 2449–2454.

[6] T. Bailey, "Constrained initialisation for bearing-only SLAM," in *Proceedings of the 2003 IEEE International Conference on Robotics and Automation*, vol. 2. IEEE, 2003, pp. 1966–1971.

[7] N. M. Kwok and G. Dissanayake, "An efficient multiple hypothesis filter for bearing-only SLAM," in *Proceedings of the 2004 IEEE/RSJ International Conference on Intelligent Robots and Systems*, vol. 1, Sept 2004, pp. 736–741.

[8] J. Solà, A. Monin, M. Devy, and T. Lemaire, "Undelayed initialization in bearing only SLAM," in *Proceedings of the 2005 IEEE/RSJ International Conference on Intelligent Robots and Systems*, Aug 2005, pp. 2499–2504.

[9] K. Bekris, M. Click, and E. Kavraki, "Evaluation of algorithms for bearing-only SLAM," in *Proceedings of the 2006 IEEE International Conference on Robotics and Automation*, May 2006, pp. 1937–1943.

[10] P. Jensfelt, D. Kragic, J. Folkesson, and M. Bjorkman, "A framework for vision based bearing only 3d slam," in *Proceedings of the 2006 IEEE International Conference on Robotics and Automation*, May 2006, pp. 1944–1950.

[11] H. Huang, F. D. Maire, and N. Keeratipranon, "Bearing-only simultaneous localization and mapping for vision-based mobile robots," in *Vision Systems-Applications*, G. Obinata and A. Dutta, Eds. Vienna, Austria: I-Tech Education and Publishing, 2007, pp. 335–360.

[12] N. Trawny and S. I. Roumeliotis, "A unified framework for nearby and distant landmarks in bearing-only SLAM," in *Proceedings of the 2006 IEEE International Conference on Robotics and Automation*. IEEE, 2006, pp. 1923–1929.

[13] P. Batista, C. Silvestre, and P. Oliveira, "Globally exponentially stable filters for source localization and navigation aided by direction measurements," *Systems & Control Letters*, vol. 62, no. 11, pp. 1065–1072, November 2013.

[14] J. Castellanos, R. Martinez-Cantin, J. Tardós, and J. Neira, "Robocentric map joining: Improving the consistency of EKF-SLAM," *Robotics and Autonomous Systems*, vol. 55, no. 1, pp. 21–29, 2007.

[15] T. Vidal-Calleja, M. Bryson, S. Sukkarieh, A. Sanfeliu, and J. Andrade-Cetto, "On the Observability of Bearing-only SLAM," in *Proceedings of the 2007 IEEE International Conference on Robotics and Automation*, April 2007, pp. 4114–4119.

[16] P. Lourenço, B. J. Guerreiro, P. Batista, P. Oliveira, and C. Silvestre, "3-D Inertial Trajectory and Map Online Estimation: Building on a GAS Sensor-based SLAM filter," in *Proc. of the 2013 European Control Conference*, Zurich, Switzerland, July 2013, pp. 4214–4219.

[17] P. Lourenço, B. J. Guerreiro, P. Batista, P. Oliveira, C. Silvestre, and C. L. P. Chen, "Sensor-based Globally Exponentially Stable Range-Only Simultaneous Localization and Mapping," *Robotics and Autonomous Systems*, vol. 68, pp. 72–85.

[18] B. J. Guerreiro, P. Batista, C. Silvestre, and P. Oliveira, "Globally Asymptotically Stable Sensor-based Simultaneous Localization and Mapping," *IEEE Transactions on Robotics*, vol. 29, no. 6, pp. 1380–1395, December 2013.

[19] P. Lourenço, B. J. Guerreiro, P. Batista, P. Oliveira, and C. Silvestre, "Preliminary Results on Globally Asymptotically Stable Simultaneous Localization and Mapping in 3-D," in *Proc. of the 2013 American Control Conference*, Washington D.C., USA, June 2013, pp. 3093–3098.

[20] P. Batista, C. Silvestre, and P. Oliveira, "Single range aided navigation and source localization: Observability and filter design," *Systems & Control Letters*, vol. 60, no. 8, pp. 665–673, 2011.

[21] R. Brockett, *Finite Dimensional Linear Systems*, ser. Series in decision and control. John Wiley & Sons, 1970.

[22] H. Khalil, *Nonlinear Systems*, 3rd ed. Prentice Hall, 2002.

[23] B. D. O. Anderson, "Stability properties of Kalman-Bucy filters," *Journal of the Franklin Institute*, vol. 291, no. 2, pp. 137–144, 1971.

[24] A. Gelb, *Applied Optimal Estimation*. MIT Press, 1974.